

# Low-energy limit of the radiative dipole strength in nuclei

Elena Litvinova

*National Superconducting Cyclotron Laboratory, Michigan State University, East Lansing, MI 48824-1321, USA*

Nikolay Belov

*Nuclear Physics Department, St. Petersburg State University, 198504 St. Petersburg, Russia*

(Dated: June 6, 2018)

We explain the low-energy anomaly reported in several experimental studies of the radiative dipole strength functions in medium-mass nuclei. These strength functions at very low gamma-energies correspond to the gamma-transitions between very close nuclear excited states in the quasicontinuum. In terms of the thermal mean-field, the low-energy enhancement of the strength functions in highly-excited compound nuclei is explained by nucleonic transitions from the thermally unblocked single-quasiparticle states to the single-(quasi)particle continuum. This result is obtained within the finite-temperature quasiparticle random phase approximation in the coordinate space with exact treatment of the single-particle continuum and exactly eliminated spurious translational mode. The case of radiative dipole strength functions at the nuclear excitation energies typical for the thermal neutron capture is illustrated for  $^{94,96,98}\text{Mo}$  and  $^{116,122}\text{Sn}$  in comparison to available data.

PACS numbers: 21.10.Pc, 21.60.Jz, 25.40.Lw, 27.60.+j

Experimental and theoretical studies of the nuclear low-energy electric dipole response remain among the challenges of the modern nuclear structure physics and attract an increasing interest because of its astrophysical impact. Radiative strength ( $\gamma$ -strength) at low energies may enhance the neutron capture rates in the r-process of nucleosynthesis [1, 2] with a considerable influence on elemental abundance distributions. One of the key phases of the r-process nucleosynthesis is capture of a thermal neutron with the subsequent  $\gamma$ -decay of the compound nucleus. The typical neutron energy in the astrophysical plasma is about 100 keV. Therefore, the description of  $\gamma$ -emission spectra of a compound nucleus with excitation energies of the order of the neutron separation energy is the central problem. Hauser-Feshbach model is a standard tool for calculations of the radiative neutron capture cross sections [3]. Formally, this model includes all possible decay channels via transmission coefficients. In the gamma-decay channel the corresponding coefficient is determined by the radiative strength function which is usually calculated by one of the phenomenological parameterizations [4–6]. However, in more recent works [1, 2, 7] it has been shown that for the most important electric dipole strength these simple models are not sufficient because they do not account for structural details of the strength at the neutron threshold. Sensitivity of the stellar reaction rates to these details emphasizes the importance of their studies within microscopic self-consistent models.

Another key ingredient for the Hauser-Feshbach calculations is the Brink-Axel hypothesis [8] stating that the  $\gamma$ -strength does not depend on the nuclear excitation energy, in particular, it is the same for excited and non-excited nuclei. Supposedly true for the giant resonances and for the soft modes like pygmy dipole resonance, this hypothesis is, however, violated for the lowest transition energies. For instance, non-zero strength is systemati-

cally observed at very low gamma-energies [9]. Radiative strength functions extracted from various measurements [10–14] show an upbend at  $E_\gamma \leq 3$  MeV in light nuclei of Fe-Mo mass region. Studies of Ref. [15] have revealed that this phenomenon, occurring in various astrophysical sites, can have a significant impact on their elemental abundances. Phenomenological approaches approximate the low-energy  $\gamma$ -strength by the tail of the giant dipole resonance with a temperature-dependent width. This is, however, not justified, because the low-energy  $\gamma$ -strength originates from underlying physics which is completely different from the giant vibrational motion. Modern microscopic theories have excellent tools for computing probabilities of transitions between the nuclear ground state and excited states, but have common problems to describe transitions between excited states. The general many-body techniques like Green function formalism [16, 17], can be applied to  $\gamma$ -emission and  $\gamma$ -absorption in excited states of compound type if it is approximated by a semi-statistical model like a finite-temperature mean-field. In such a case, the transitions are described by the finite-temperature version of the random-phase approximation and its extensions. There exist formulations within discrete model spaces [18–20] and models with exact treatment of the single-particle continuum [21–24].

In this paper, we explain the mechanism for the enhancement of the low-frequency dipole  $\gamma$ -transitions between the nuclear excited states in the quasicontinuum. We show, for the first time, that this phenomenon can be quantitatively described in terms of a microscopic many-body approach built on the thermal mean-field description of the compound nucleus. Exact treatment of single-particle continuum at finite temperature and exact elimination of the center-of-mass motion are the two essential ingredients for understanding these dipole  $\gamma$ -transitions with frequencies  $E_\gamma \leq 3$ -4 MeV.

The general concept of the finite-temperature mean-

field theory [18, 19, 25] is based on the variational principle of maximum entropy minimizing the thermodynamical potential

$$\Omega(\lambda, T) = E - \lambda N - TS, \quad (1)$$

with the Lagrange multipliers  $\lambda$  and  $T$  determined by the average energy  $E$ , particle number  $N$  and the entropy  $S$ . These quantities are the thermal averages involving the generalized one-body density operator  $\mathcal{R}$ :

$$S = -k\text{Tr}(\mathcal{R}\ln\mathcal{R}), \quad E = \text{Tr}(\mathcal{R}\mathcal{H}), \quad N = \text{Tr}(\mathcal{R}\mathcal{N}), \quad (2)$$

where  $\mathcal{H}$  is the nuclear Hamiltonian,  $\mathcal{N}$  is the particle number operator, and  $k$  is Boltzmann constant. Varying the Eq. (1), one can determine the density operator  $\mathcal{R}$  with the unity trace:

$$\mathcal{R} = \frac{e^{-(\mathcal{H}-\lambda\mathcal{N})/kT}}{\text{Tr}\left[e^{-(\mathcal{H}-\lambda\mathcal{N})/kT}\right]}, \quad \mathcal{H} = \frac{\delta E[\mathcal{R}]}{\delta \mathcal{R}}. \quad (3)$$

For definiteness, we start from a spherical even-even compound nucleus with spin and parity  $0^+$ .  $\gamma$ -emission and  $\gamma$ -absorption are described as an interaction of the nucleus with a sufficiently weak external electromagnetic field  $P$  oscillating with some frequency  $\omega$ . The interaction with such a field causes small amplitude nuclear oscillations around the static equilibrium, so that the total density matrix  $\mathcal{R}$  has an oscillating term, in addition to the static thermal mean-field part  $\mathcal{R}^0$ :

$$\mathcal{R}(t) = \mathcal{R}^0 + [\delta\mathcal{R}e^{-i\omega t} + h.c.]. \quad (4)$$

Variation  $\delta\mathcal{R}$  of the density matrix  $\mathcal{R}$  in the external field  $P$  obeys, in the local approximation, the following integral equation:

$$\delta\mathcal{R}(x; \omega, T) = \delta\mathcal{R}^{(0)}(x; \omega, T) + \int dx' dx'' \mathcal{A}(x, x'; \omega, T) F(x', x'') \delta\mathcal{R}(x''; \omega, T), \quad (5)$$

where  $x$  is a multi-index  $x = \{\mathbf{r}, s, \tau, \chi\}$  of spatial coordinate  $\mathbf{r}$ , spin  $s$ , isospin  $\tau$  and component in the quasiparticle space  $\chi$ .  $F(x, x')$  is the effective nucleon-nucleon interaction,  $\mathcal{A}(x, x'; \omega, T)$  is the two-quasiparticle propagator in the nuclear medium at finite temperature and

$$\delta\mathcal{R}^{(0)}(x; \omega, T) = \int dx' \mathcal{A}(x, x'; \omega, T) P(x'). \quad (6)$$

The propagator  $\mathcal{A}(x, x'; \omega, T)$  is the key quantity and ideally has to include all the in-medium and surface effects. In the first approximation we calculate it within the thermal continuum quasiparticle random phase approximation (TCQRPA) in terms of the Matsubara temperature Green functions [16, 17]. The full expression of the TCQRPA propagator in the coordinate space is presented in [23], for the case of spherical symmetry. The propagator consists of the discrete and continuum

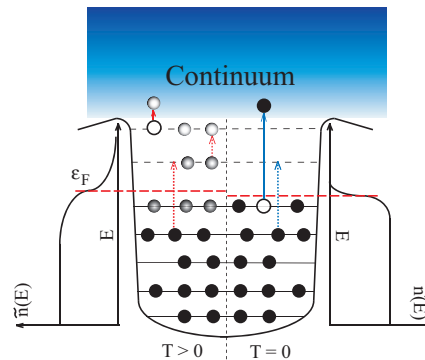


FIG. 1: Schematic picture of the possible lowest-energy single-quasiparticle transitions from the thermally unblocked states in an excited compound (left) and from the "frozen" ones in the ground-state nucleus (right).

parts. The discrete part describes transitions between the single-quasiparticle states in the discrete spectrum, and the continuum part describes transitions from the discrete spectrum states to the continuum. Dashed and solid arrows in Fig. 1 show the low-frequency transitions of both kinds, respectively. For the case of  $\gamma$ -emission, the arrows indicate photons while nucleons transit back to lower-energy orbits. For the absorption the situation is reversed. The effective occupation probability distribution  $\tilde{n}_i(E_i, T)$  has much larger diffuseness at finite  $T$  than at  $T=0$ , being the following product:  $\tilde{n}_i(E_i, T) = v_i^2(T)(1 - n_i(E_i, T))$  below the Fermi energy  $\varepsilon_F$ , and  $\tilde{n}_i(E_i, T) = (1 - v_i^2(T))n_i(E_i, T)$  above  $\varepsilon_F$ ,  $v_i$  are the occupation numbers of Bogoliubov quasiparticles,

$$n_i(E_i, T) = \frac{1}{1 + \exp(E_i(T)/kT)}, \quad (7)$$

and  $E_i$  are the eigenvalues of the single-particle Hamiltonian. The mean-field is generated by the Woods-Saxon (WS) potential and the effective nucleon-nucleon interaction  $F(x, x')$  has the Landau-Migdal ansatz. The dipole radiative strength function (RSF) corresponding to the  $0^+ \rightarrow 1^-$  transition is determined by the quantity  $\delta\mathcal{R}$  through its convolution with the electromagnetic dipole operator  $P_{E1}(x) = e^{\tau r} Y_1(\mathbf{r})$  with effective charges  $e^n = -Z/A$ ,  $e^p = N/A$ :

$$f_{E1}(E_\gamma, T) = -\frac{8e^2}{27(\hbar c)^3} \text{Im} \int dx P_{E1}^\dagger(x) \delta\mathcal{R}(x; \omega, T), \quad (8)$$

$\omega = E_\gamma + i\Delta$ ,  $\Delta \rightarrow 0$ . Formally, Eq. (8) corresponds to  $\gamma$ -absorption, and  $\gamma$ -emission strength can be calculated for the "final temperature"  $T_f = \sqrt{(E^* - \delta - E_\gamma)/a}$  [26]. However, for  $E_\gamma \leq 3-4$  MeV the  $\gamma$ -absorption and  $\gamma$ -emission strength functions are close to each other. Their differences will be discussed elsewhere.

The elimination of the spurious state associated with the broken translation invariance is performed by means of the "forced consistency" technique described in Ref. [27] and generalized to the finite temperature case. Due to the special terms in the effective interaction, the Goldstone mode sets at exactly zero energy and has zero tran-

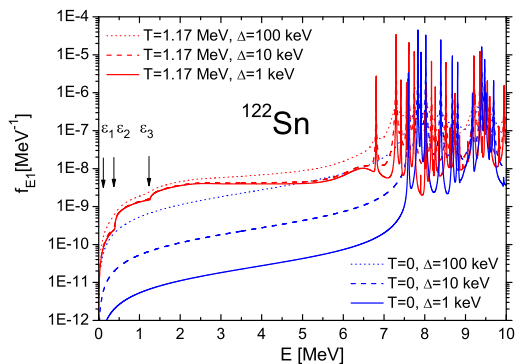


FIG. 2: Radiative dipole strength in  $^{122}\text{Sn}$  calculated within TCQRPA with different smearing parameters, see text for details.

sition probability. Fig. 2 shows the radiative dipole strength in  $^{122}\text{Sn}$  at finite and zero temperature computed with diminishing smearing parameters  $\Delta$ , so that the absence of admixture of the Goldstone mode is clearly demonstrated. Moreover, while at  $T=0$  the low-energy strength is just an artificial tail of the first excited state of the discrete spectrum, at finite temperature the low-energy strength has the pure continuum origin and practically saturated at  $\Delta = 10$  keV. At this and smaller values of  $\Delta$  the finite-temperature strength at low energies shows steps at the energies equal to the energies of the single-particle states closest to the continuum  $\varepsilon_i = \varepsilon_F + E_i$ , that confirms the interpretation given by Fig. 1. For the illustration we have selected some nuclei for which the dipole RSF have been studied recently and reported in Refs. [11, 28, 29]. Figs. 3 and 4 display the dipole RSF in  $^{94,96,98}\text{Mo}$  and  $^{116,122}\text{Sn}$  calculated within the TCQRPA at finite and zero temperatures, compared to data. To be specific, in this work we consider the nuclear excitation energy  $E^*$  equal to the neutron separation energy  $E^* = S_n$ . The corresponding temperature parameter  $T$  is determined from the phenomenological relation  $T = \sqrt{(E^* - \delta)/a}$ , where  $\delta$  is the so-called back shift and  $a$  is the level density parameter. For both  $\delta$  and  $a$  there are no universal values. The numerical values for  $\delta$  are taken from Ref. [30]. For  $a$  we have taken the values from the enhanced generalized superfluid model [30] as upper limits and the lower limits are obtained microscopically from the single-particle level densities of neutrons  $g_\nu$  and protons  $g_\pi$  in the WS potential as  $a = \pi^2(g_\nu + g_\pi)/6$ . Thus, the intervals of relevant temperatures vary from nucleus to nucleus as  $1.26 \leq T \leq 1.59$ ;  $1.15 \leq T \leq 1.55$ ;  $1.02 \leq T \leq 1.52$  MeV for  $^{94,96,98}\text{Mo}$  and  $1.03 \leq T \leq 1.3$ ,  $1.02 \leq T \leq 1.17$  MeV for  $^{116,122}\text{Sn}$ , respectively. The uncertainty in determining the temperature parameter corresponds to the uncertainty in the data normalization discussed in Ref. [15] for Mo isotopes. The colored bands in Fig. 3 bordered by the strengths at minimal and maximal temperature parameters can be compared with data obtained with both normalization procedures and agree reasonably within the bands, however, the uncertainties for the temperature are too large to be in favor of a particular normalization. While the dash-dotted

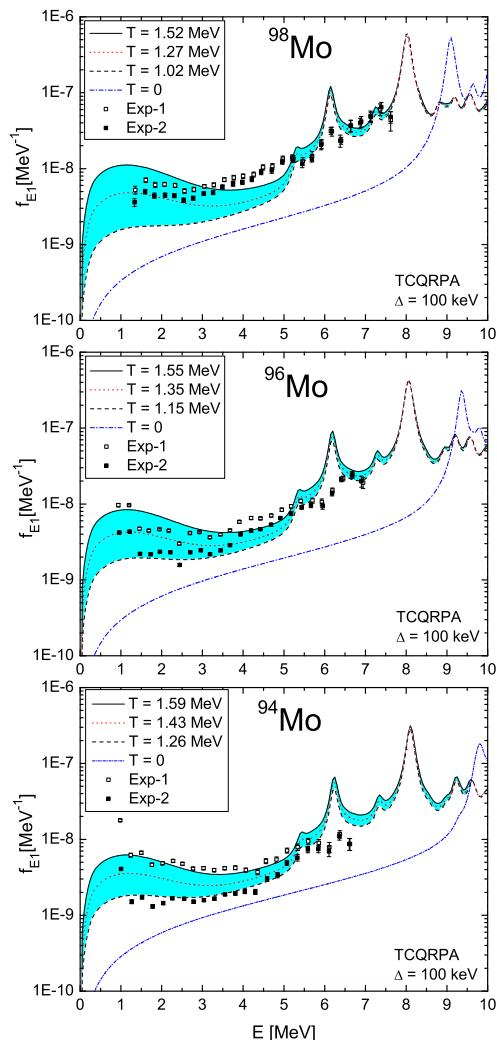


FIG. 3: The E1  $\gamma$ -strength functions for even-even Mo isotopes at finite temperatures obtained within the TCQRPA, compared to data [11] and to the  $\gamma$ -strength for the ground state ( $T=0$ , dash-dotted curves).

blue curves ( $T=0$ ) show at low  $\gamma$ -energies the tails of the higher-energy transitions only due to the non-zero value of  $\Delta$ , at finite  $T$  there is the pure thermal continuum strength which remains finite at  $\Delta \rightarrow 0$ , as explained in Fig. 2. This means that the low-energy strength has the origin which is completely different from the high-frequency nuclear oscillations. The results obtained for odd-even Mo isotopes are similar to that for the even-even ones and on the same level of agreement to data. The RSF in  $^{116,122}\text{Sn}$  show no upbends at the relevant temperatures (pink bands in Fig. 4) because their upper limits are smaller than in Mo isotopes due to the larger WS values of  $a$ . The results are consistent with data below 4-5 MeV. The red dotted curves show how the RSF develops at higher temperature.

Fig. 1 gives a qualitative interpretation for the low-energy enhancement of the  $\gamma$ -strength. It is clearly seen that transitions from the thermally unblocked states of the single-particle spectrum to the continuum (solid ar-

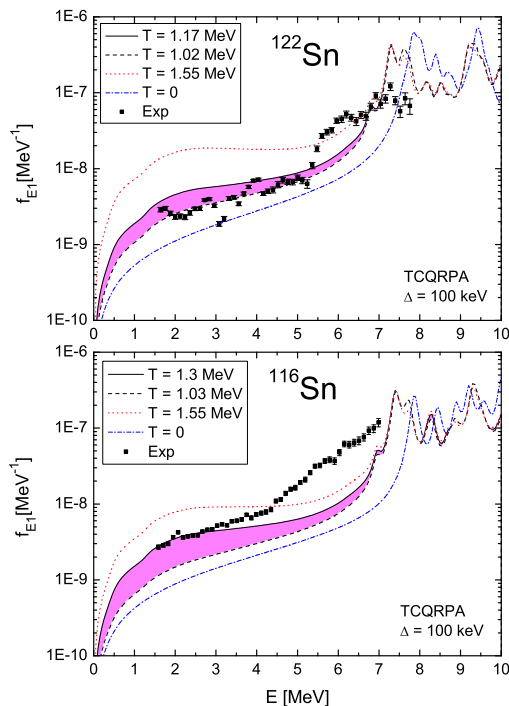


FIG. 4: Same as in Fig. 3, but for  $^{116,122}\text{Sn}$ , compared to data from Refs. [28, 29].

row in Fig. 1, left part  $T > 0$ ) form solely the  $\gamma$ -strength function at very low transition frequency  $E_\gamma$ . Such type of transitions is not possible in the ground state ( $T=0$ ) where the lowest-energy transitions to the continuum have much higher energies (solid arrow in Fig. 1, right part). This schematic picture also explains why the low-energy RSF grows with temperature, however, the numerical calculations show that the precise behavior of the strength depends on the particular details of the single-

particle structure.

Although the thermal QRPA with exact continuum treatment explains the main mechanism of formation of the  $\gamma$ -strength at low energies, other mechanisms can further modify the strength. Coupling to complex configurations [31, 32] and thermal fluctuations [33] cause resonance-like structures on the strength functions at energies above 4-5 MeV. These effects at finite temperatures should be included in the future work.

Summarizing, we give a theoretical interpretation of the low-energy anomaly in the behavior of the radiative dipole strength in medium-mass and heavy nuclei. We have shown that a microscopic approach to nuclear response with coupling to the continuum and exactly eliminated center-of-mass motion, based on the statistical description of the compound nucleus, gives a very good approximation to the low-energy  $\gamma$ -strength already on the level of the two-quasiparticle configurations. Application to electric dipole response explains the systematic low-energy enhancement of the  $\gamma$ -strength on the microscopic level. Thus, it is shown that microscopic nuclear many-body theory can be brought to the domain which was previously dominated by phenomenological approaches. The obtained results may have an important consequence for astrophysics, namely for the approaches to r-process nucleosynthesis: those involving Brink-Axel hypothesis may need to be revised.

The authors are indebted to H. Feldmeier, Yu. Ivanov, E. Kolomeitsev, G. Martínez-Pinedo, V. Tselyaev and V. Zelevinsky for enlightening discussions. Support from Helmholtz Alliance EMMI and from NSCL (E.L.), from GSI Summer Student Program 2009 and from the St. Petersburg State University under Grant No. 11.38.648.2013 (N.B.) is gratefully acknowledged.

- 
- [1] S. Goriely and E. Khan, Nucl. Phys. **A706**, 217 (2002).  
[2] S. Goriely, E. Khan, and M. Samyn, Nucl. Phys. **A739**, 331 (2004).  
[3] J.J. Cowan, F.-K. Thielemann, J.W. Truran, Phys. Rep. **208**, 267 (1991).  
[4] S.G. Kadenskii, V.P. Markushev, V.I. Furman, Yad. Fiz. **37**, 277 (1983), Sov. J. Nucl. Phys. **37**, 165 (1983).  
[5] J. Kopecky, M. Uhl, Phys. Rev. C **41**, 1941 (1990).  
[6] S.F. Mughabghab, C.L. Dunford, Phys. Lett. B **487**, 155 (2000).  
[7] E. Litvinova *et al.* Nucl. Phys. **A823**, 26 (2009).  
[8] D. Brink, Ph.D. thesis, Oxford University, 1955.  
[9] A. Schiller, M. Thoennessen, Atomic Data and Nuclear Data Tables **93**, 549 (2007).  
[10] A. Voinov *et al.*, Phys. Rev. Lett. **93**, 142504.  
[11] M. Guttormsen *et al.*, Phys. Rev. C **71**, 044307 (2005).  
[12] A. C. Larsen *et al.*, Phys. Rev. C **76**, 044303 (2007).  
[13] E. Algin *et al.*, Phys. Rev. C **78**, 054321 (2008).  
[14] M. Wiedeking *et al.*, Phys. Rev. Lett. **108**, 162503.  
[15] A.C. Larsen, S. Goriely, Phys. Rev. C **82**, 014318 (2010).  
[16] T. Matsubara, Prog. Theor. Phys. **14**, 351 (1955).  
[17] A.A. Abrikosov, L.P. Gorkov, I.E. Dzyaloshinski, *Methods of Quantum Field Theory in Statistical Physics*, Prentice-Hall, 1963.  
[18] P. Ring *et al.*, Nucl. Phys. **A419**, 261 (1983).  
[19] H.M. Sommermann, Ann. Phys. **151**, 163 (1983).  
[20] Y.F. Niu *et al.*, Phys. Lett. B **681**, 315 (2009).  
[21] J. Bar-Touv, Phys. Rev. C **32**, 1369 (1985).  
[22] V.A. Rodin, M.G. Urin, PEPAN **31**, 975 (2000).  
[23] E.V. Litvinova, S.P. Kamerdzhiev, V.I. Tselyaev, Yad. Fiz. **66**, 584 (2003); Phys. Atomic Nuclei **66**, 558 (2003).  
[24] E. Khan, N. Van Giai, M. Grasso, Nucl. Phys. **A731**, 311 (2004).  
[25] A.L. Goodman, Nucl. Phys. **A352**, 30 (1981).  
[26] V.A. Plujko, Nucl. Phys. **A649**, 209c (1999).  
[27] S. Kamerdzhiev *et al.*, Phys. Rev. C **58**, 172 (1998).  
[28] H.K. Toft *et al.*, Phys. Rev. C **81**, 064311 (2010).  
[29] H.K. Toft *et al.*, Phys. Rev. C **83**, 044320 (2011).  
[30] <http://www-nds.iaea.org/RIPL-3/>.  
[31] E. Litvinova, P. Ring, V. Tselyaev, Phys. Rev. C **78**, 014312 (2008).  
[32] V. Tselyaev *et al.*, Phys. Rev. C **75**, 014315 (2007).

[33] M. Gallardo *et al.*, Nucl. Phys. **A443**, 415 (1985).